Trap loss in a rubidium crossed dipole trap by short-range photoassociation

Carlos R. Menegatti,[1] Bruno S. Marangoni,[1] Nadia Bouloufa-Maafa,[2] Olivier Dulieu,[2] and Luis G. Marcassa[1]
[1]*Instituto de Física de São Carlos, Universidade de São Paulo, Caixa Postal 369, 13560-970 São Carlos, SP, Brazil*
[2]*Laboratoire Aimé Cotton, CNRS/Université Paris-Sud/ENS Cachan, Bâtiment 505, Campus d'Orsay, F-91405 Orsay, France*
(Received 3 January 2013; published 8 May 2013)

Significant two-body losses are observed in an ultracold gas of ^{85}Rb or ^{87}Rb atoms in a crossed dipole trap implemented with a broadband laser with a wavelength around 1071 nm. Using available spectroscopic data on the excited states of Rb_2, as well as accurate computed transition dipole moment functions, we interpret these losses as due to photoassociation of deeply bound levels of the 0_u^+ coupled states by the trapping laser, followed by spontaneous emission down to bound levels of the Rb_2 ground state thus forming ultracold molecules. The observed ratio of 3.3 between the loss rates of ^{87}Rb and ^{85}Rb is well reproduced by the theoretical model.

DOI: 10.1103/PhysRevA.87.053404 PACS number(s): 34.50.Rk, 34.10.+x, 32.80.Rm

I. INTRODUCTION

Ultracold molecules have attracted special attention in recent years because they are expected to have a significant impact on different research fields, such as Bose-Einstein condensation, ultracold chemistry, quantum information, and precision metrology [1–6]. However, the production of such molecules, at temperatures below 1 mK, is still challenging, mainly because it requires several steps. The first step is to obtain a large and dense sample of cold trapped atoms. The second step involves most often the formation of molecules in a weakly bound rovibrational level of the ground-state manifold, which can be accomplished by performing either the photoassociation process or Feshbach resonance, or a combination of both [1–6]. At the end of this step, the molecular sample can be either in a thermal regime [7–11] or a quantum regime [12,13]. The final step is the preparation of the sample in a single vibrational state, which can be done either by stimulated Raman adiabatic passage (STIRAP) [12,13] or optical pumping [14].

An optical dipole trap can be a valuable tool for the molecule formation process for several reasons: (i) It allows the production of dense atomic samples, from which the molecules are formed; (ii) the trapping mechanism does not depend on molecular or atomic levels, nor does it interfere with the production of the molecule or its vibrational state preparation; and finally (iii) it is able to confine molecules, allowing studies involving atom-molecule and molecule-molecule collisions. Nowadays, high-power fiber lasers around 1060 nm are a reliable and inexpensive tool for such studies. Although its wavelength is far away from the $D2$ line of alkaline atoms (such as K, Rb, and Cs), it could in principle access excited molecular levels at short range. Such a short-range photoassociation process has already been observed in the formation of cold RbCs molecules in a magneto-optical trap [15]. In an optical dipole trap, Sofikitis and co-workers [16] were the first to point out that such a process could happen due to a 1060 nm dipole trap laser in a Cs sample. Lauber and co-workers [17] have partially investigated the same process in a broadband optical dipole trap for a Rb sample.

In this paper, we study the time evolution of ^{85}Rb and ^{87}Rb atoms trapped in a crossed optical dipole trap created by a broadband 1071 nm fiber laser. The decay curve for both isotopes presents a nonexponential behavior, which suggests the existence of density-dependent losses. We have ruled out thermalization, the three-body recombination process, and hyperfine changing collision as possible explanations for such losses. A theoretical model based on short-range photoassociation due to the broadband laser at 1071 nm was implemented, which considers the singlet electronic ground-state potential $X\,^1\Sigma_g^+$ and the excited potentials $b\,^3\Pi_u$ and $A\,^1\Sigma_u^+$. The theoretical model is able to reproduce the isotope difference observed in the experiment, and it also predicts that molecules should be formed in electronic ground-state potential $X\,^1\Sigma_g^+$. Investigation of such ultracold molecules is underway.

II. EXPERIMENTAL SETUP

Our magneto-optical trap (MOT) operates in a stainless chamber with a background pressure below 10^{-10} torr, and it is loaded from a Zeeman-slowed atomic beam. The chamber design is very similar to that in Ref. [18]. In our setup, we can cool and trap either ^{85}Rb or ^{87}Rb atoms. We start from a standard MOT, which traps about 10^8 atoms at an atomic density of 2×10^{10} cm^{-3}. For ^{85}Rb, the trapping laser beam was tuned to the red of the $5S_{1/2}(F = 3) \rightarrow 5P_{3/2}(F' = 4)$ atomic transition and the repumping laser beam was tuned to the $5S_{1/2}(F = 2) \rightarrow 5P_{3/2}(F' = 3)$ atomic transition. For ^{87}Rb, the trapping laser beam was tuned to the red of the $5S_{1/2}(F = 2) \rightarrow 5P_{3/2}(F' = 3)$ line and the repumping laser beam was tuned to the $5S_{1/2}(F = 1) \rightarrow 5P_{3/2}(F' = 2)$ atomic transition. At the MOT conditions, independently of the chosen isotope, the trapping laser intensity per arm was $I_T = 8$ mW/cm^2 and detuning was $\Delta_T \simeq -3.4\Gamma$, where $\Gamma = 2\pi \times 5.9$ MHz; the repumping laser intensity per arm was $I_R \simeq 1.6$ mW/cm^2 and with a detuning $\Delta_R = 0$. The optical dipole trap is provided by a randomly polarized broadband fiber laser at 1071 nm (IPG Photonics model YLR-40-1070, full width at half-maximum of 1.5 nm), which is focused into the MOT volume with a waist of 125 ± 15 μm at an available power of 25 W at 1071 nm (single beam peak intensity $\sim$103 kW/cm^2, corresponding to a maximum total trap depth of $\sim$150 μK). The same laser beam was recycled to create the crossed trapping region. The laser beam waist was obtained by measuring the axial ($\omega_{ax}/2\pi = 0.6 \pm 0.2$ Hz) and radial ($\omega_{rad}/2\pi = 210 \pm 40$ Hz) oscillation frequencies in

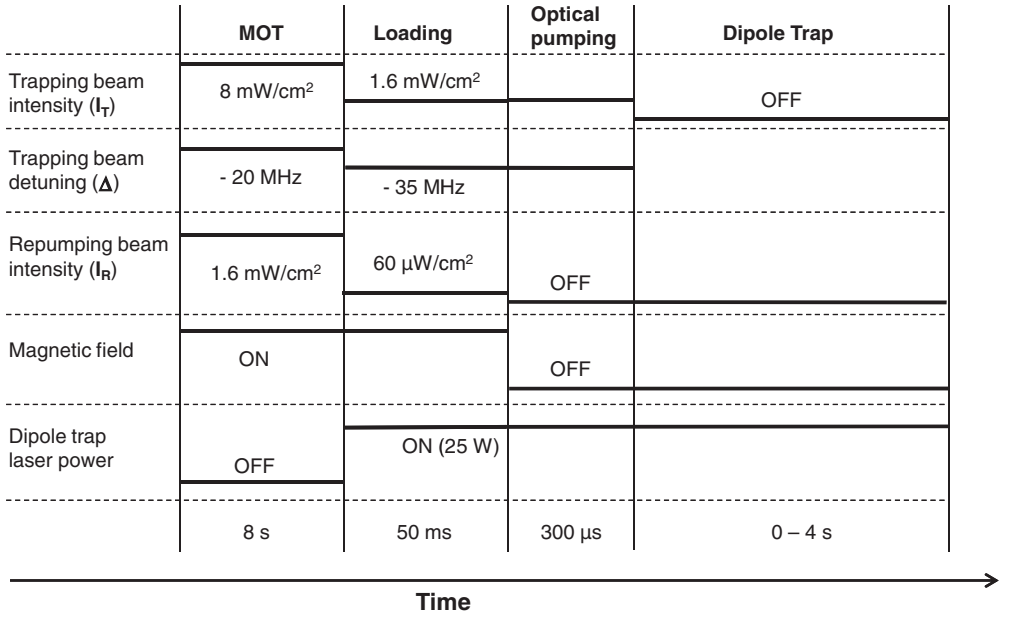

FIG. 1. Experimental time sequence. The dipole trap phase maybe varied from 0 up to 4 s.

each independent single beam dipole trap [19]. The experiment runs according to the following time sequence (shown in Fig. 1): (i) a MOT loading phase, whose duration is about 8 s, consisting of both trapping and repumping laser beams at the initial MOT conditions. The optical dipole trap remains off. (ii) An optical dipole trap loading phase, whose duration is 50 ms. In this phase, the dipole trap beam is turned on and the intensity and frequency of the trapping and repumping lasers are varied to loading conditions ($I_T = 1.6$ mW/cm^2, $\Delta_T \simeq -6\Gamma$, $I_R \simeq 60$ μW/cm^2, and $\Delta_R = 0$). (iii) In the sequence, there is an optical pumping phase, in which the magnetic field gradient is turned off in 100 μs, and a delay time of 300 μs between the turning off of the trapping and repumping laser beams allows us to optically pump the atoms to different hyperfine levels of the atomic ground state. If the trapping laser is turned off before the repumping laser, the atomic sample will be pumped to the $F = 2$ hyperfine ground state for ^{87}Rb (or the $F = 3$ hyperfine ground state for ^{85}Rb). If the repumping laser is turned off before the trapping laser, the atomic sample will be pumped to the $F = 1$ hyperfine ground state for ^{87}Rb (or the $F = 2$ hyperfine ground state for ^{85}Rb). (iv) Finally, there is the dipole trap phase, in which a pure atomic sample is held in the dipole trap in a specific hyperfine ground state, however it is not polarized. The residual magnetic field at this phase is less than 0.1 G. To characterize the purity of the sample, we have turned off the dipole trap and applied a state-selective absorption imaging technique, which relies on two absorption images: (i) In the first image, the imaging laser beam is on the cycling transition $5S_{1/2}(F = 3) \rightarrow 5P_{3/2}(F' = 4)$ for ^{85}Rb [or $5S_{1/2}(F = 2) \rightarrow 5P_{3/2}(F' = 3)$ for ^{87}Rb] without additional repumping light. Therefore, only atoms in the higher hyperfine ground state are able to absorb such light, which allows us to obtain the population in such a state ($F = 3$ for ^{85}Rb or $F = 2$ for ^{87}Rb). (ii) In the sequence, we repeat this measurement with repumping light, which allows us to obtain the total number of trapped atoms and therefore the purity of the sample. According to our measurements, the purity of the sample is larger than 99%. By varying the holding time in the dipole trap, we are able to obtain the time evolution of the atomic population using absorption imaging. At the initial typical conditions, we have about $(3.0 \pm 0.3) \times 10^6$ trapped atoms at a density of $(4.0 \pm 1.2) \times 10^{12}$ cm^{-3}. The sample's temperature was obtained by ballistic expansion using the absorption imaging technique.

III. EXPERIMENTAL RESULTS

Figure 2 shows the experimental results for the time evolution of the atom number in the dipole trap (N) for both isotopes prepared in the lower hyperfine ground state, $F = 1$ for ^{87}Rb and $F = 2$ for ^{85}Rb, respectively. Each experimental point is an average of five independent measurements, and presents a 7% error bar due to the variance of all measurements. In the inset of Fig. 2, we show the measured temperature as a function of trapping time, which we found to be time-independent and around 30 $\pm$ 10 μK. Clearly, the atomic population decay curves cannot be fitted by a single exponential decay, suggesting that density-dependent losses do occur in our sample. Since the atoms are in the lower hyperfine ground state, we shall consider first the three-body recombination process as a possible explanation. However, we have estimated its contribution to the atom loss rate as 10^6 and 10^3 atoms/s at $t = 0$ (highest density) for ^{85}Rb and ^{87}Rb, respectively [20–22]. Such an estimation cannot account for the measured atom loss rate of about 2×10^7 atoms/s for both isotopes, and therefore the three-body recombination process can be ruled out. Another possibility is thermalization in the dipole trap [23]; however, we have estimated its contribution to be less than 10^6 atoms/s at $t = 0$ (highest density) for either isotope [24]. Besides, the sample's temperature should decrease, which is not observed in our experiment. In a recent work by Lauber and co-workers [17], the authors associated part of such losses to a hyperfine

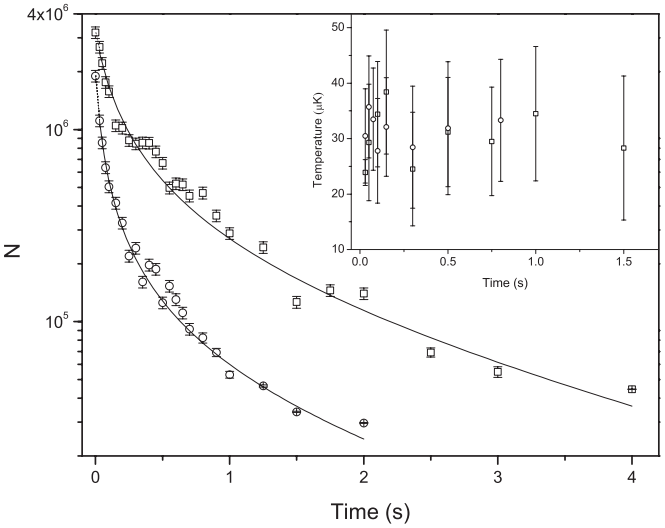

FIG. 2. Atom number in the dipole trap N for ^{87}Rb (circles) and ^{85}Rb (squares). The points are experimental results and the lines are a fitting using Eq. (3). Each experimental point is an average of five independent measurements, and presents a 7% error bar due to their variance. The inset shows the measured temperature as a function of trapping time, which is time-independent and around 30 ± 10 μK.

changing collision in the ground state. According to them, the broad linewidth of the dipole trap laser was responsible for pumping atoms to the upper hyperfine ground state, leading to collisions and losses. We tried to observe such optical pumping in our system by using state-selective absorption imaging; however, the population in the upper hyperfine ground state was always below 1% at any time for both isotopes when the sample was prepared in the lower hyperfine ground state. This observation leads us to believe that we are observing collisions only between lower hyperfine ground-state atoms. For this reason, we have described the evolution of the atom population in the dipole trap using a two-body loss rate equation for the atomic density n:

$$\frac{dn}{dt} = -\gamma n - \beta n^2, \tag{1}$$

where γ is due to background losses involving collisions between hot and cold atoms, and β is due to collisions between cold atoms. From our absorption images, we have observed that our atomic density has a Gaussian spatial profile, which can be given by $n(r) = n_0 \exp(-x^2/2w^2 - y^2/2w^2 - z^2/2w_z^2)$, where w and w_z are the sample waists parallel and perpendicular to the dipole trap plane. Such an effect is due to the anisotropy of the potential of a crossed dipole trap [19]. Therefore, if we integrate Eq. (1) over the entire atomic sample, the time evolution of N is given by

$$\frac{dN}{dt} = -\gamma N - \frac{\beta}{8\pi^{3/2} w^2 w_z} N^2, \tag{2}$$

the solution of which is

$$N(t) = \frac{N_0 e^{-\gamma t}}{1 + \left(\frac{N_0 \beta}{8\pi^{3/2} w^2 w_z \gamma}\right)(1 - e^{-\gamma t})}, \tag{3}$$

TABLE I. Experimental two-body loss rate obtained for all hyperfine levels of the atomic ground state of both isotopes trapped in the 1071 nm dipole trap.

Atomic state	n (10^{12} cm^{-3})	β (10^{-12} cm^3/s)
^{85}Rb		
$F = 2$	4.0 ± 1.2	3.2 ± 0.9
$F = 3$	5.3 ± 1.2	5.2 ± 1.5
^{87}Rb		
$F = 1$	4.0 ± 1.2	10.6 ± 3.2
$F = 2$	4.0 ± 1.2	12 ± 4

where N_0 is the number of atoms at $t = 0$. By fitting the experimental decay curves, using Eq. (3), we have obtained all the free parameters for all the hyperfine levels of the atomic ground state of both isotopes. From the absorption images, we have also obtained $w = 52 \pm 5$ μm ($w_z = 36 \pm 4$ μm) for ^{87}Rb and $w = 62 \pm 5$ μm ($w_z = 45 \pm 5$ μm) for ^{85}Rb, respectively. In Table I, we present the experimental two-body loss rates for all hyperfine levels of the atomic ground state.

From Table I, we can notice that the difference between the lower and the upper hyperfine ground-state loss rate for both isotopes is about 10^{-12} cm^3/s. Although such a difference is on the order of our error bar, we believe that it might be associated with a hyperfine change collision taking place in the upper hyperfine ground state, since the purity of the sample is about 99%. Unfortunately, all the hyperfine changing collision measurements for Rb were performed in a MOT, where resonant light is known to play an important role [25]. Nevertheless, the theory presented in this work [25] predicts a loss rate due to hyperfine change collisions around 10^{-12} cm^3/s for ^{87}Rb occurring in the absence of resonant light at 30 μK temperature. The same theory was applied for Cs and it was in good agreement with experimental results obtained in a CO_2 dipole trap [26], which gives us a fair amount of confidence in our comparison. Such an observation also rules out a hyperfine changing collision due to broadband optical pumping as responsible for the observed losses in the lower hyperfine ground state.

We were puzzled by the absence of optical pumping to the upper hyperfine ground state in our setup. Therefore, we decided to increase the intensity of the 1071 nm light by decreasing the waist of the dipole laser beam and increasing the available total power. For the new conditions, we had a waist of 65 μm at an available power of 40 W at 1071 nm (single beam peak intensity ~600 kW/cm^2, corresponding to a maximum total trap depth of ~880 μK). Under such conditions, we were able to observe the optical pumping for both isotopes. Figure 3(a) shows the fraction of atoms in the upper hyperfine ground state (F_{uh}) for both isotopes as a function of trapping time. We have observed similar population transfer to that in Ref. [17] due to optical pumping, however at a light intensity that is two times larger. The main difference between both setups is the 1070 nm laser. Our crossed dipole trap has a random polarization, and both dipole laser beams have the same frequency and a smaller bandwidth. Another important observation is that the optical pumping for ^{85}Rb is about three times smaller than for ^{87}Rb. The reason for such a difference is unknown, but this is beyond the scope of this work.

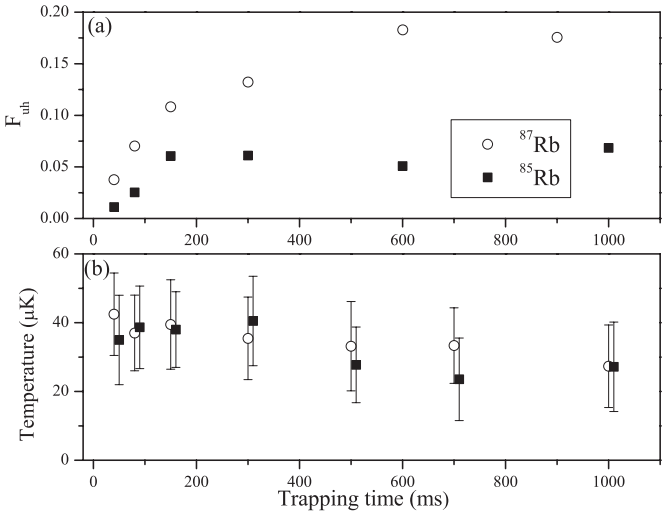

FIG. 3. (a) Fraction of atoms in the upper hyperfine ground state (F_{uh}) as a function of trapping time for both isotopes for a 600 KW/cm^2 peak intensity at 1071 nm. (b) Atomic temperature as a function of trapping time.

The atomic temperature as a function of trapping time was also measured at this new configuration [Fig. 3(b)], and it was found to be around 35 ± 10 μK, independent of trapping time. This result is consistent with the fact that hyperfine changing collisions are not important in our experiment. Because the hyperfine splitting of the Rb ground state exceeds by far the depth of the trapping potential, it causes the two inelastically colliding atoms to be lost from the trap. So, if such a process was playing a major role, we would observe a temperature increase as the trapping time increases, as was observed for Cs [26]. Therefore, we believe such a collision process can be ruled out in our experiment.

IV. PA AND COLD MOLECULE FORMATION WITH THE TRAPPING BROADBAND LASER

To explain the observed collisional losses, we have considered a theoretical model based on photoassociation (PA) due to the trapping broadband laser at 1071 nm. The proposed processes are schematized in Fig. 4. A pair of colliding cold atoms in the $X\,^1\Sigma_g^+$ ground state [27] is photoassociated by the 1071 nm trapping laser into vibrational levels of the coupled $A\,^1\Sigma_u^+$ and $b\,^3\Pi_u$ electronic states interacting via diagonal and off-diagonal R-dependent spin-orbit interaction

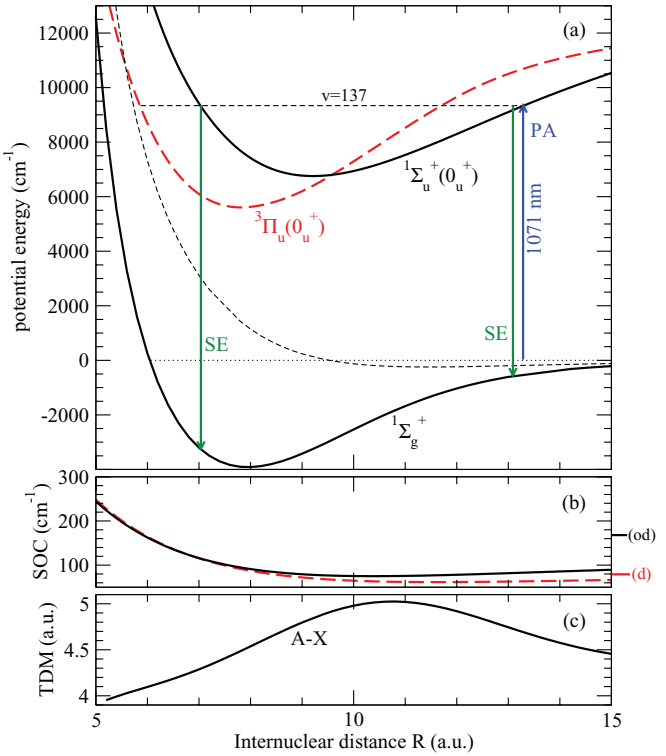

FIG. 4. (Color online) Scheme of the proposed cold molecule formation process. (a) Relevant potential curves taken from the experimental determinations of Ref. [27] for the $X\,^1\Sigma_g^+$ ground state, and from Ref. [28] for the $A\,^1\Sigma_u^+$ and $b\,^3\Pi_u$ states. The ^{87}Rb$_2$ 0_u^+ bound level $v = 137$ presumably reached by PA with the 1070 nm laser is indicated. Downward arrows suggest the Franck-Condon points for which spontaneous emission (SE) down to the X state is expected to be favored. (b) The diagonal (red dashed line) and off-diagonal (black full line) spin-orbit couplings (SOC) between the A and b states as determined in Ref. [28], with their respective atomic limit indicated by the (d) and (od) labels. (c) Transition dipole moment (TDM) between the A and X state, reported in Ref. [29].

[Fig. 4(b)], giving rise to a pair of 0_u^+ coupled states (in Hund's case, c) [28]. The $a\,^3\Sigma_u^+$ ground state is not considered here because there is no dipole-allowed transition to the A/b excited states. The strength of the transition is controlled by the transition dipole moment D_{XA} between the X and A states [Fig. 4(c)] [29]. To perform reliable calculations of both continuum and bound-state wave functions, we extrapolated the A and b potential curves at large distances

TABLE II. Properties of the 0_u^+ vibrational levels v' excited by the trapping laser for both isotopologues, recomputed from the supplementary material of Ref. [28]: the binding energy $E_{v'}$ (in cm^{-1}, relative to the $5S + 5P$ asymptote), the transition energy (in cm^{-1}, relative to the $5S + 5S$ asymptote), the rotational constant $B_{v'}$ (in cm^{-1}), the fraction (normalized to 1) of their wave function on the b and A electronic states, the excitation wavelength, and the value of the squared TDM (in arbitrary units) with the initial colliding state at 30 μK. The energy difference between the $5S + 5S$ and the $5S + 5P$ asymptotes is 12 737.34 cm^{-1}.

	v'	$E_{v'}$	$T_{v'}$	$B_{v'}$	b component	A component	$\lambda_{v'}$	(TDM)^2
^{85}Rb$_2$	135	−3416.4	9320.9	0.01828	0.7587	0.2412		
	136	−3396.4	9340.9	0.01494	0.1257	0.8742	1070.55 nm	0.1876×10^{-6}
^{87}Rb$_2$	137	−3411.8	9325.5	0.01804	0.0989	0.9011	1072.33 nm	0.1020×10^{-5}
	138	−3385.5	9351.8	0.0145	0.7939	0.2061		

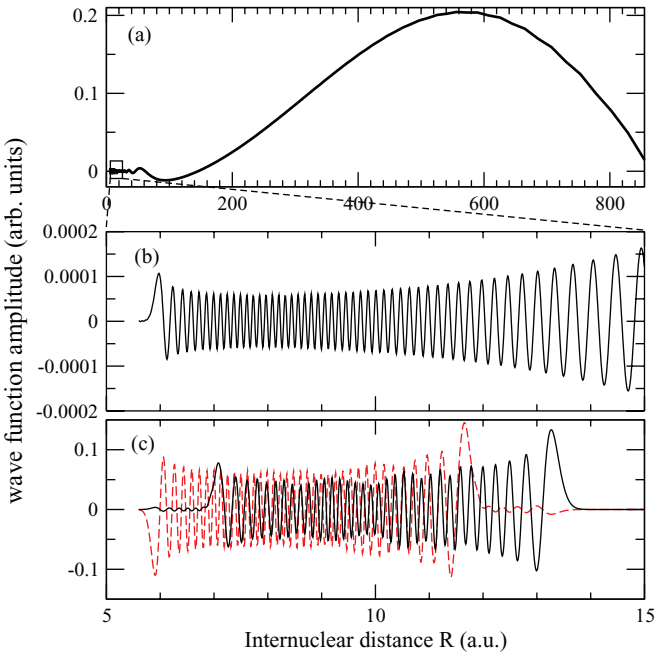

FIG. 5. (Color online) (a) Radial wave function of a colliding ^{85}Rb atom pair at ϵ/k_B= 30 μK in the ground-state potential $X\,^1\Sigma_g^+$. (b) Blow-up of the wave function in (a) at short internuclear distances. (c) Radial components on the $A\,^1\Sigma_u^+$ (full black line) and $b\,^3\Pi_u$ (dashed red line) electronic states of the wave function of the vibrational level $\nu' = 136$ of the 0_u^+ coupled states.

with a C_m/R^m expansion ($m = 3,6$) with the asymptotic coefficients C_m taken from Ref. [30]. The radial wave functions are evaluated using the mapped Fourier grid Hamiltonian method (see Refs. [31,32] for details), which has been proven to be very convenient in the case of coupled electronic states.

Due to the large bandwidth (17 cm^{-1}), two vibrational levels ν' of the 0_u^+ coupled states can be excited for each isotopologue ^{85}Rb$_2$ and ^{87}Rb$_2$ (Table II). Note that the label ν' refers to the numbering of vibrational levels of the coupled 0_u^+ states, and not of the individual A or b states. In each case, one level with a predominant component on the A state can be populated, and an example of the related radial wave function is displayed in Fig. 5 for ^{87}Rb$_2$. The rates for the PA transition and for the spontaneous emission are determined by the squared transition dipole moments $|\langle X;\epsilon|D_{XA}|0_u^+(A);\nu'\rangle|^2$ and $|\langle X;\nu''|D_{XA}|0_u^+(A);\nu'\rangle|^2$, respectively. In these expressions, $|X;\epsilon\rangle$, $|0_u^+;\nu'\rangle$, and $|X;\nu''\rangle$ are the radial wave functions for the initial colliding state with temperature $\epsilon/k_B = 30$ μK for the A component of the populated 0_u^+ level ν', and for levels ν'' of the X state. Results for ^{85}Rb$_2$ are displayed in Fig. 6, and a similar pattern is obtained for ^{87}Rb$_2$. In both cases, we considered the level which has the dominant A character, namely $\nu' = 136$ and 137 for ^{85}Rb$_2$ and ^{87}Rb$_2$, respectively. These levels are not the most efficient for the PA transition, but they are predicted to decay almost entirely (>95%) into bound levels of the X state, thus yielding ultracold ground-state molecules in a broad range of vibrational levels above $\nu'' \approx 20$ [see Fig. 6(b)].

The computation of PA rates can be performed using the perturbative theory developed in Ref. [33] yielding a rate

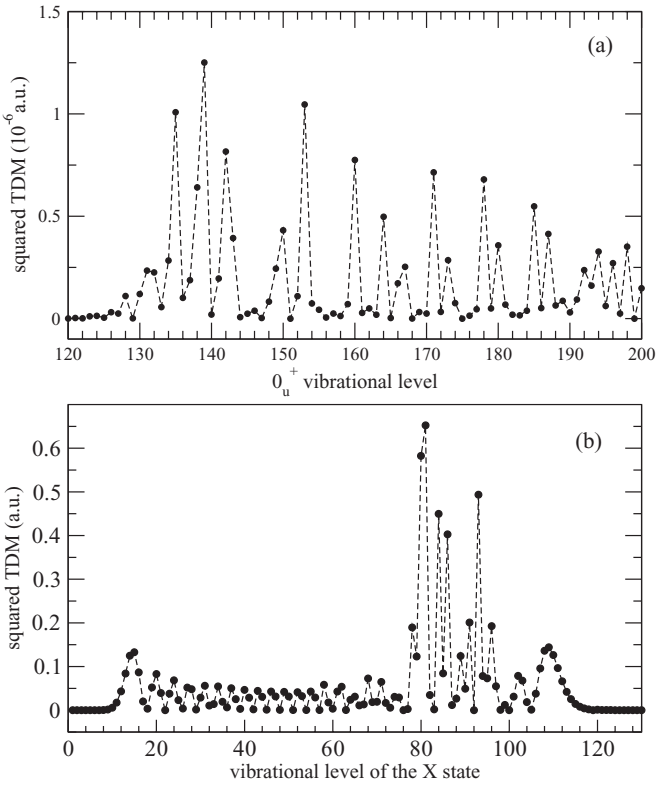

FIG. 6. Squared transition dipole moment (TDM) of the transitions relevant to this work for ^{85}Rb: (a) Between the ground-state scattering wave function at 30 μK of Fig. 5(a) and the $A\,^1\Sigma_u^+$ component of the bound vibrational wave functions of the 0_u^+ coupled states; (b) between the 0_u^+ ($\nu' = 136$) wave function of Fig. 5(c) and the wave functions of the $X\,^1\Sigma_g^+$ vibrational levels.

proportional to the squared TDM and to the laser intensity available for the absorption. The determination of the relevant laser intensity is tedious in the present case due to the large power and broad width of the trapping laser. Its intensity density is assumed with a Gaussian shape according to $I(\lambda) = I_0\exp[-(\lambda-\lambda_c)^2/\Delta\lambda^2]$, where $I_0 = 0.102$ MW/cm^2 nm, $\lambda_c = 1071.3$ nm, and $\Delta\lambda = 1.096$ nm. We should point out that the total intensity considered here is the contribution of both dipole trap beams. Considering that the levels with dominant A character above are responsible for the loss signal, we can estimate the ratio of the corresponding PA rates $R_{\rm PA}$ between the two isotopologues from the data reported in Table II and by picking the laser intensity $I(\lambda)$ at the wavelength appropriate for the considered levels. We thus obtain that $R_{\rm PA}(^{87}{\rm Rb};\nu' = 137)/R_{\rm PA}(^{85}{\rm Rb};\nu' = 136) = 4.1$, in reasonable agreement with the observed value of 3.3. This measured ratio thus reflects the difference between the TDM of the photoassociated levels, weighted by the available laser intensity $I(\lambda)$ at their excitation wavelength.

V. CONCLUSION

In conclusion, we have measured the time evolution of ^{85}Rb and ^{87}Rb atoms trapped in a crossed optical dipole trap created by a broadband 1071 nm fiber laser. The decay curve for both isotopes presents a nonexponential behavior, which

suggests the existence of density-dependent losses. We have ruled out the three-body recombination process and hyperfine changing collision as possible explanations for such losses. A theoretical model based on photoassociation due to the broadband laser at 1071 nm was implemented, which considers the singlet electronic ground-state potential $X\,^1\Sigma_g^+$ and the $b\,^3\Pi_u$ and $A\,^1\Sigma_u^+$ excited potentials. The agreement between the theoretical model and the experimental results is excellent. The model also predicts that molecules should be formed in the electronic ground-state potential $X\,^1\Sigma_g^+$. Investigation of such molecules is underway.

ACKNOWLEDGMENT

This work is supported by FAPESP (Fundação de Amparo á Pesquisa do Estado de São Paulo), INCT-IQ, and CNPq.

[1] Reviews in *Cold Molecules: Theory, Experiment, Applications*, edited by R. V. Krems, W. C. Stwalley, and B. Friedrich (CRC, Boca Raton, FL, 2009).
[2] M. A. Baranov, Phys. Rep. **464**, 71 (2008).
[3] T. Lahaye, C. Menotti, L. Santos, M. Lewenstein, and T. Pfau, Rep. Prog. Phys. **72**, 126401 (2009).
[4] L. D. Carr, D. DeMille, R. V. Krems, and J. Ye, New J. Phys. **11**, 055049 (2009).
[5] B. Friedrich and J. M. Doyle, ChemPhysChem **10**, 604 (2009).
[6] O. Dulieu and C. Gabbanini, Rep. Prog. Phys. **72**, 086401 (2009).
[7] N. Zahzam, T. Vogt, M. Mudrich, D. Comparat, and P. Pillet, Phys. Rev. Lett. **96**, 023202 (2006).
[8] T. Takekoshi, B. M. Patterson, and R. J. Knize, Phys. Rev. Lett. **81**, 5105 (1998).
[9] P. Staanum, S. D. Kraft, J. Lange, R. Wester, and M. Weidemuller, Phys. Rev. Lett. **96**, 023201 (2006).
[10] E. R. Hudson, N. B. Gilfoy, S. Kotochigova, J. M. Sage, and D. DeMille, Phys. Rev. Lett. **100**, 203201 (2008).
[11] A. Fioretti, J. Lozeille, C. A. Massa, M. Mazzoni, and C. Gabbanini, Opt. Commun. **243**, 203 (2004).
[12] K.-K. Ni, S. Ospelkaus, M. H. G. de Miranda, A. Pe'er, B. Neyenhuis, J. J. Zirbel, S. Kotochigova, P. S. Julienne, D. S. Jin, and J. Ye, Science **322**, 231 (2008).
[13] J. G. Danzl, E. Haller, M. Gustavsson, M. J. Mark, R. Hart, N. Bouloufa, O. Dulieu, H. Ritsch, and H. C. Nagerl, Science **321**, 1062 (2008).
[14] M. Viteau, A. Chotia, M. Allegrini, N. Bouloufa, O. Dulieu, D. Comparat, and P. Pillet, Science **321**, 232 (2008).
[15] C. Gabbanini and O. Dulieu, Phys. Chem. Chem. Phys. **13**, 18905 (2011).
[16] D. Sofikitis, G. Stern, L. Kime, E. Dimova, A. Fioretti, D. Comparat, and P. Pillet, Eur. Phys. J. D **61**, 437 (2011).
[17] T. Lauber, J. Kuber, O. Wille, and G. Birkl, Phys. Rev. A **84**, 043641 (2011).
[18] E. W. Streed, A. P. Chikkatur, T. L. Gustavson, M. Boyd, Y. Torii, D. Schneble, G. K. Campbell, D. E. Pritchard, and W. Ketterle, Rev. Sci. Instrum. **77**, 023106 (2006); C. R. Menegatti, B. S. Marangoni, and L. G. Marcassa, Phys. Rev. A **84**, 053405 (2011).
[19] R. Grimm, M. Weidemüller, and Y. B. Ovchinnikov, Adv. At. Mol. Opt. Phys. **42**, 95 (2000).
[20] C. Gabbanini, A. Fioretti, A. Lucchesini, S. Gozzini, and M. Mazzoni, Phys. Rev. Lett. **84**, 2814 (2000).
[21] E. A. Burt, R. W. Ghrist, C. J. Myatt, M. J. Holland, E. A. Cornell, and C. E. Wieman, Phys. Rev. Lett. **79**, 337 (1997).
[22] C. H. Greene (private communication).
[23] H. Engler, T. Weber, M. Mudrich, R. Grimm, and M. Weidemuller, Phys. Rev. A **62**, 031402(R) (2000).
[24] O. J. Luiten, M. W. Reynolds, and J. T. M. Walraven, Phys. Rev. A **53**, 381 (1996); K. M. O'Hara, M. E. Gehm, S. R. Granade, and J. E. Thomas, *ibid.* **64**, 051403(R) (2001).
[25] S. D. Gensemer, P. L. Gould, P. J. Leo, E. Tiesinga, and C. J. Williams, Phys. Rev. A **62**, 030702 (2000).
[26] M. Mudrich, S. Kraft, J. Lange, A. Mosk, M. Weidemuller, and E. Tiesinga, Phys. Rev. A **70**, 062712 (2004).
[27] J. Y. Seto, R. J. Le Roy, J. Vergés, and C. Amiot, J. Chem. Phys. **113**, 3067 (2000).
[28] H. Salami, T. Bergeman, B. Beser, J. Bai, E. H. Ahmed, S. Kotochigova, A. M. Lyyra, J. Huennekens, C. Lisdat, A. V. Stolyarov, O. Dulieu, P. Crozet, and A. J. Ross, Phys. Rev. A **80**, 022515 (2009).
[29] R. Beuc, M. Movre, V. Horvatic, C. Vadla, O. Dulieu, and M. Aymar, Phys. Rev. A **75**, 032512 (2007).
[30] M. Marinescu and A. Dalgarno, Phys. Rev. A **52**, 311 (1995).
[31] V. Kokoouline, O. Dulieu, and F. Masnou-Seeuws, Phys. Rev. A **62**, 022504 (2000).
[32] V. Kokoouline, J. Vala, and R. Kosloff, J. Chem. Phys. **114**, 3046 (2001).
[33] P. Pillet, A. Crubellier, A. Bleton, O. Dulieu, P. Nosbaum, I. Mourachko, and F. Masnou-Seeuws, J. Phys. B **30**, 2801 (1997).